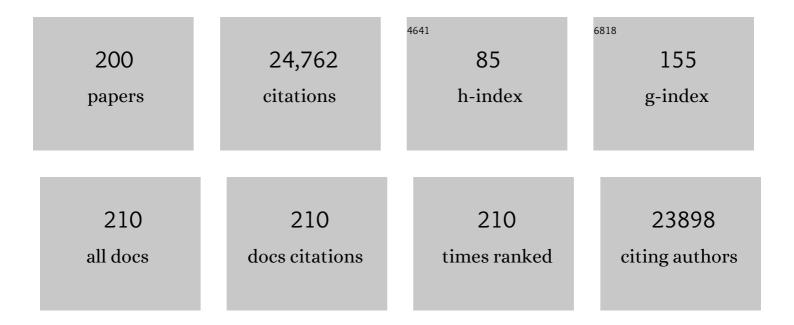
Ling-Dong Sun

List of Publications by Year in descending order

Source: https://exaly.com/author-pdf/4625043/publications.pdf Version: 2024-02-01



#	Article	IF	CITATIONS
1	An Extraâ€Broadband VISâ€NIR Emitting Phosphor toward Multifunctional LED Applications. Advanced Functional Materials, 2022, 32, .	7.8	59

2 An Extraâ€Broadband VISâ€NIR Emitting Phosphor toward Multifunctional LED Applications (Adv. Funct.) Tj ETQq0.0,0 rgBT /Overlock 1

3	Upconverted/downshifted NaLnF4 and metal-organic framework heterostructures boosting NIR-II imaging-guided photodynamic immunotherapy toward tumors. Nano Today, 2022, 43, 101439.	6.2	43
4	Allâ€Inorganic Manganeseâ€Based CsMnCl ₃ Nanocrystals for Xâ€Ray Imaging. Advanced Science, 2022, 9, e2201354.	5.6	37
5	Migrating photon avalanche in different emitters at the nanoscale enables 46th-order optical nonlinearity. Nature Nanotechnology, 2022, 17, 524-530.	15.6	63
6	Design, Identification, and Evolution of a Surface Ruthenium(II/III) Single Site for CO Activation. Angewandte Chemie, 2021, 133, 1232-1239.	1.6	0
7	Design, Identification, and Evolution of a Surface Ruthenium(II/III) Single Site for CO Activation. Angewandte Chemie - International Edition, 2021, 60, 1212-1219.	7.2	8
8	An overview of rare earth coupled lead halide perovskite and its application in photovoltaics and light emitting devices. Progress in Materials Science, 2021, 120, 100737.	16.0	35
9	Networking State of Ytterbium Ions Probing the Origin of Luminescence Quenching and Activation in Nanocrystals. Advanced Science, 2021, 8, 2003325.	5.6	31
10	Desilylation Induced by Metal Fluoride Nanocrystals Enables Cleavage Chemistry In Vivo. Journal of the American Chemical Society, 2021, 143, 2250-2255.	6.6	16
11	Upconversion Fluorescence Resonance Energy Transfer Aptasensors for H5N1 Influenza Virus Detection. ACS Omega, 2021, 6, 15236-15245.	1.6	19
12	Lanthanide Upconverted Microlasing: Microlasing Spanning Full Visible Spectrum to Nearâ€Infrared under Low Power, CW Pumping. Small, 2021, 17, e2103140.	5.2	7
13	Highly Polarized Upconversion Emissions from Lanthanide-Doped LiYF ₄ Crystals as Spatial Orientation Indicators. Journal of Physical Chemistry Letters, 2021, 12, 11288-11294.	2.1	14
14	Local Structure Engineering in Lanthanide-Doped Nanocrystals for Tunable Upconversion Emissions. Journal of the American Chemical Society, 2021, 143, 20546-20561.	6.6	62
15	Improvement in the stability of γ-CsPbI ₃ nanowires enabled by lattice immobilization through the Pb–O anchor in SBA-15. Inorganic Chemistry Frontiers, 2020, 7, 4572-4579.	3.0	4
16	Intrinsically Active Surface in a Pt/γ-Mo ₂ N Catalyst for the Water–Gas Shift Reaction: Molybdenum Nitride or Molybdenum Oxide?. Journal of the American Chemical Society, 2020, 142, 13362-13371.	6.6	41
17	Adsorption and activation of molecular oxygen over atomic copper(I/II) site on ceria. Nature Communications, 2020, 11, 4008.	5.8	95
18	Upconversion emission studies of single particles. Nano Today, 2020, 35, 100956.	6.2	50

#	Article	IF	CITATIONS
19	Carrier transport composites with suppressed glass-transition for stable planar perovskite solar cells. Journal of Materials Chemistry A, 2020, 8, 14106-14113.	5.2	18
20	Engineering of Upconverted Metal–Organic Frameworks for Near-Infrared Light-Triggered Combinational Photodynamic/Chemo-/Immunotherapy against Hypoxic Tumors. Journal of the American Chemical Society, 2020, 142, 3939-3946.	6.6	294
21	Experimental and Simulation Insights into Local Structure and Luminescence Evolution in Eu ³⁺ -Doped Nanocrystals under High Pressure. Journal of Physical Chemistry Letters, 2020, 11, 3515-3520.	2.1	20
22	Lanthanide-Doped Upconversion Nanoparticles for Super-Resolution Microscopy. Frontiers in Chemistry, 2020, 8, 619377.	1.8	28
23	Facile synthesis of Au embedded CuOx-CeO2 core/shell nanospheres as highly reactive and sinter-resistant catalysts for catalytic hydrogenation of p-nitrophenol. Nano Research, 2020, 13, 2044-2055.	5.8	39
24	Crystallization of Gd ₂ O ₃ nanoparticles: evolution of the microstructure <i>via</i> electron-beam manipulation. Nanoscale, 2019, 11, 14952-14958.	2.8	2
25	Regulation of the cellular uptake of nanoparticles by the orientation of helical polypeptides. Nano Research, 2019, 12, 889-896.	5.8	14
26	Direct Identification of Active Surface Species for the Water–Gas Shift Reaction on a Gold–Ceria Catalyst. Journal of the American Chemical Society, 2019, 141, 4613-4623.	6.6	139
27	A Eu ³⁺ -Eu ²⁺ ion redox shuttle imparts operational durability to Pb-I perovskite solar cells. Science, 2019, 363, 265-270.	6.0	793
28	Nanophotonic energy storage in upconversion nanoparticles. Nano Energy, 2019, 56, 473-481.	8.2	43
29	Scalable Direct Writing of Lanthanide-Doped KMnF ₃ Perovskite Nanowires into Aligned Arrays with Polarized Up-Conversion Emission. Nano Letters, 2018, 18, 2964-2969.	4.5	52
30	Nanobubble-embedded inorganic 808Ânm excited upconversion nanocomposites for tumor multiple imaging and treatment. Chemical Science, 2018, 9, 3141-3151.	3.7	53
31	Chitosan-coated cerium oxide nanocubes accelerate cutaneous wound healing by curtailing persistent inflammation. Inorganic Chemistry Frontiers, 2018, 5, 386-393.	3.0	67
32	Measuring Activation and Luminescence Time Scales of Upconverting NaYF ₄ :Yb,Er Nanocrystals. Journal of Physical Chemistry C, 2018, 122, 23780-23789.	1.5	6
33	Pt-Embedded CuO _{<i>x</i>} –CeO ₂ Multicore–Shell Composites: Interfacial Redox Reaction-Directed Synthesis and Composition-Dependent Performance for CO Oxidation. ACS Applied Materials & Interfaces, 2018, 10, 34172-34183.	4.0	29
34	Phase segregation enabled scandium fluoride–lanthanide fluoride Janus nanoparticles. Inorganic Chemistry Frontiers, 2018, 5, 1800-1804.	3.0	5
35	Compositionâ€Graded Cesium Lead Halide Perovskite Nanowires with Tunable Dual olor Lasing Performance. Advanced Materials, 2018, 30, e1800596.	11.1	99
36	Composition-tuned oxidation levels of Pt–Re bimetallic nanoparticles for the etherification of allylic alcohols. Nano Research, 2018, 11, 5902-5912.	5.8	3

#	Article	IF	CITATIONS
37	Investigations on multi-photon emissions of Nd 3+ -sensitized core/shell nanoparticles. Journal of Rare Earths, 2017, 35, 1-6.	2.5	13
38	Versatile Spectral and Lifetime Multiplexing Nanoplatform with Excitation Orthogonalized Upconversion Luminescence. ACS Nano, 2017, 11, 3289-3297.	7.3	237
39	Minimizing the Heat Effect of Photodynamic Therapy Based on Inorganic Nanocomposites Mediated by 808 nm Nearâ€Infrared Light. Small, 2017, 13, 1700038.	5.2	94
40	Self-sacrificed two-dimensional REO(CH ₃ COO) template-assisted synthesis of ultrathin rare earth oxide nanoplates. Inorganic Chemistry Frontiers, 2017, 4, 1182-1186.	3.0	5
41	Photodynamic Therapy: Minimizing the Heat Effect of Photodynamic Therapy Based on Inorganic Nanocomposites Mediated by 808 nm Nearâ€Infrared Light (Small 21/2017). Small, 2017, 13, .	5.2	0
42	Interface formation energy, bonding, energy band alignment in α-NaYF 4 related core shell models: For future multi-layer core shell luminescence materials. Journal of Rare Earths, 2017, 35, 315-334.	2.5	7
43	Gd-Dots with Strong Ligand–Water Interaction for Ultrasensitive Magnetic Resonance Renography. ACS Nano, 2017, 11, 3642-3650.	7.3	84
44	Ultralow-power near-infrared excited neodymium-doped nanoparticles for long-term in vivo bioimaging. Nanoscale, 2017, 9, 4660-4664.	2.8	44
45	Heterogeneous synergistic catalysis by Ru-RuO x nanoparticles for Se–Se bond activation. Nano Research, 2017, 10, 922-932.	5.8	18
46	<i>In situ</i> epitaxial growth of GdF ₃ on NaGdF ₄ :Yb,Er nanoparticles. Inorganic Chemistry Frontiers, 2017, 4, 2119-2125.	3.0	4
47	Design and validation of a new ratiometric intracellular pH imaging probe using lanthanide-doped upconverting nanoparticles. Dalton Transactions, 2017, 46, 13957-13965.	1.6	27
48	Heterodimers Made of Upconversion Nanoparticles and Metal–Organic Frameworks. Journal of the American Chemical Society, 2017, 139, 13804-13810.	6.6	147
49	A-Site Cation Effect on Growth Thermodynamics and Photoconductive Properties in Ultrapure Lead Iodine Perovskite Monocrystalline Wires. ACS Applied Materials & Interfaces, 2017, 9, 25985-25994.	4.0	14
50	Moderate oxidation levels of Ru nanoparticles enhance molecular oxygen activation for cross-dehydrogenative-coupling reactions via single electron transfer. RSC Advances, 2017, 7, 33078-33085.	1.7	14
51	Selective Cation Exchange Enabled Growth of Lanthanide Core/Shell Nanoparticles with Dissimilar Structure. Journal of the American Chemical Society, 2017, 139, 18492-18495.	6.6	83
52	Unravelling the energy transfer of Er ³⁺ -self-sensitized upconversion in Er ³⁺ –Yb ³⁺ –Er ³⁺ clustered core@shell nanoparticles. Nanoscale, 2017, 9, 18490-18497.	2.8	10
53	NIR Ratiometric Luminescence Detection of pH Fluctuation in Living Cells with Hemicyanine Derivative-Assembled Upconversion Nanophosphors. Analytical Chemistry, 2017, 89, 8863-8869.	3.2	65
54	Pt-embedded-CeO ₂ hollow spheres for enhancing CO oxidation performance. Materials Chemistry Frontiers, 2017, 1, 1754-1763.	3.2	36

#	Article	IF	CITATIONS
55	Recent Progress in Wellâ€Controlled Synthesis of Ceriaâ€Based Nanocatalysts towards Enhanced Catalytic Performance. Advanced Energy Materials, 2016, 6, 1600501.	10.2	115
56	Photon upconversion in Yb ³⁺ –Tb ³⁺ and Yb ³⁺ –Eu ³⁺ activated core/shell nanoparticles with dual-band excitation. Journal of Materials Chemistry C, 2016, 4, 4186-4192.	2.7	52
57	Silicon Oxycarbide/Carbon Nanohybrids with Tiny Silicon Oxycarbide Particles Embedded in Free Carbon Matrix Based on Photoactive Dental Methacrylates. ACS Applied Materials & Interfaces, 2016, 8, 13982-13992.	4.0	36
58	Ceria-Based Nanocatalysts: Recent Progress in Well-Controlled Synthesis of Ceria-Based Nanocatalysts towards Enhanced Catalytic Performance (Adv. Energy Mater. 17/2016). Advanced Energy Materials, 2016, 6, .	10.2	1
59	Fundamental View of Electronic Structures of β-NaYF ₄ , β-NaGdF ₄ , and β-NaLuF ₄ . Journal of Physical Chemistry C, 2016, 120, 18858-18870.	1.5	42
60	Lanthanide Nanoparticles. Fundamental Theories of Physics, 2016, , 301-335.	0.1	3
61	Thickness Control Produces Gold Nanoplates with Their Plasmon in the Visible and Nearâ€Infrared Regions. Advanced Optical Materials, 2016, 4, 76-85.	3.6	91
62	A Versatile Imaging and Therapeutic Platform Based on Dual-Band Luminescent Lanthanide Nanoparticles toward Tumor Metastasis Inhibition. ACS Nano, 2016, 10, 2766-2773.	7.3	131
63	Hydrophilic CeO ₂ nanocubes protect pancreatic β-cell line INS-1 from H ₂ O ₂ -induced oxidative stress. Nanoscale, 2016, 8, 7923-7932.	2.8	32
64	Template-free synthesis of titania architectures with controlled morphology evolution. Journal of Materials Science, 2016, 51, 3941-3956.	1.7	8
65	Porous titania/carbon hybrid microspheres templated by in situ formed polystyrene colloids. Journal of Colloid and Interface Science, 2016, 469, 242-256.	5.0	5
66	Noble metal plasmonic nanostructure related chromisms. Inorganic Chemistry Frontiers, 2016, 3, 203-217.	3.0	12
67	TbF3 nanoparticles as dual-mode contrast agents for ultrahigh field magnetic resonance imaging and X-ray computed tomography. Nano Research, 2016, 9, 1135-1147.	5.8	33
68	Luminescenceâ€Driven Reversible Handedness Inversion of Selfâ€Organized Helical Superstructures Enabled by a Novel Nearâ€Infrared Light Nanotransducer. Advanced Materials, 2015, 27, 2065-2069.	11.1	225
69	Upconversion of Rare Earth Nanomaterials. Annual Review of Physical Chemistry, 2015, 66, 619-642.	4.8	127
70	Rare Earth Based Anisotropic Nanomaterials: Synthesis, Assembly, and Applications. Nanoscience and Technology, 2015, , 157-208.	1.5	0
71	Engineering the defect state and reducibility of ceria based nanoparticles for improved anti-oxidation performance. Nanoscale, 2015, 7, 13981-13990.	2.8	100
72	Multifunctional upconversion–nanoparticles–trismethylpyridylporphyrin–fullerene nanocomposite: a near-infrared light-triggered theranostic platform for imaging-guided photodynamic therapy. NPG Asia Materials, 2015, 7, e205-e205.	3.8	84

#	Article	IF	CITATIONS
73	Lanthanide Nanoparticles: From Design toward Bioimaging and Therapy. Chemical Reviews, 2015, 115, 10725-10815.	23.0	946
74	Solvothermal synthesis of hierarchical Eu ₂ O ₃ nanostructures templated by PS-b-PMAA: morphology control via simple variation of water contents. Journal of Materials Chemistry A, 2015, 3, 5789-5793.	5.2	7
75	PAA-capped GdF3 nanoplates as dual-mode MRI and CT contrast agents. Science Bulletin, 2015, 60, 1092-1100.	4.3	34
76	Efficient Tailoring of Upconversion Selectivity by Engineering Local Structure of Lanthanides in Na _{<i>x</i>} REF _{3+<i>x</i>} Nanocrystals. Journal of the American Chemical Society, 2015, 137, 6569-6576.	6.6	154
77	Facile Scalable Synthesis of TiO ₂ /Carbon Nanohybrids with Ultrasmall TiO ₂ Nanoparticles Homogeneously Embedded in Carbon Matrix. ACS Applied Materials & Interfaces, 2015, 7, 24247-24255.	4.0	36
78	Energy transfer in lanthanide upconversion studies for extended optical applications. Chemical Society Reviews, 2015, 44, 1608-1634.	18.7	859
79	Photon energy upconversion through thermal radiation with the power efficiency reaching 16%. Nature Communications, 2014, 5, 5669.	5.8	111
80	Green Facile Scalable Synthesis of Titania/Carbon Nanocomposites: New Use of Old Dental Resins. ACS Applied Materials & Interfaces, 2014, 6, 18461-18468.	4.0	38
81	Porous Pd nanoparticles with high photothermal conversion efficiency for efficient ablation of cancer cells. Nanoscale, 2014, 6, 4345-4351.	2.8	139
82	Reversible Near-Infrared Light Directed Reflection in a Self-Organized Helical Superstructure Loaded with Upconversion Nanoparticles. Journal of the American Chemical Society, 2014, 136, 4480-4483.	6.6	257
83	Paradigms and Challenges for Bioapplication of Rare Earth Upconversion Luminescent Nanoparticles: Small Size and Tunable Emission/Excitation Spectra. Accounts of Chemical Research, 2014, 47, 1001-1009.	7.6	324
84	Nd ³⁺ -Sensitized Upconversion Nanophosphors: Efficient <i>In Vivo</i> Bioimaging Probes with Minimized Heating Effect. ACS Nano, 2013, 7, 7200-7206.	7.3	786
85	Double shelled hollow nanospheres with dual noble metal nanoparticle encapsulation for enhanced catalytic application. Nanoscale, 2013, 5, 9747.	2.8	62
86	TWO-DIMENSIONAL AND THREE-DIMENSIONAL CERIA-BASED NANOARCHITECTURES. Catalytic Science Series, 2013, , 295-359.	0.6	1
87	Generalized Synthesis of Mesoporous Rare Earth Oxide Thin Films through Amphiphilic Ionic Block Copolymer Templating. European Journal of Inorganic Chemistry, 2013, 2013, 1251-1257.	1.0	8
88	Construction of NaREF4-based binary and bilayer nanocrystal assemblies. Chemical Communications, 2013, 49, 5799.	2.2	12
89	Basic understanding of the lanthanide related upconversion emissions. Nanoscale, 2013, 5, 5703.	2.8	203
90	Plasmonic Harvesting of Light Energy for Suzuki Coupling Reactions. Journal of the American Chemical Society, 2013, 135, 5588-5601.	6.6	597

#	Article	IF	CITATIONS
91	Time–Temperature Indicator for Perishable Products Based on Kinetically Programmable Ag Overgrowth on Au Nanorods. ACS Nano, 2013, 7, 4561-4568.	7.3	173
92	Nanorods-assembled CeVO4 hollow spheres as active catalyst for oxidative dehydrogenation of propane. Materials Research Bulletin, 2013, 48, 1122-1127.	2.7	32
93	SnO2–ZnSn(OH)6: a novel binary affinity probe for global phosphopeptide detection. Chemical Communications, 2013, 49, 1762.	2.2	48
94	Novel TiO2–Pt@SiO2 nanocomposites with high photocatalytic activity. Nanoscale, 2012, 4, 3242.	2.8	41
95	Interfacial growth behavior of SnO2 nanorods on {112̄0} and {101̄0} facets of α-Fe2O3. Nanoscale, 2012, 4, 5092.	2.8	8
96	Improving Hematite's Solar Water Splitting Efficiency by Incorporating Rare-Earth Upconversion Nanomaterials. Journal of Physical Chemistry Letters, 2012, 3, 3188-3192.	2.1	98
97	Plasmonic Percolation: Plasmon-Manifested Dielectric-to-Metal Transition. ACS Nano, 2012, 6, 7162-7171.	7.3	89
98	Porous Singleâ€Crystalline Palladium Nanoparticles with High Catalytic Activities. Angewandte Chemie - International Edition, 2012, 51, 4872-4876.	7.2	206
99	Selective Heteroepitaxial Nanocrystal Growth of Rare Earth Fluorides on Sodium Chloride: Synthesis and Density Functional Calculations. Angewandte Chemie - International Edition, 2012, 51, 8796-8799.	7.2	28
100	Rareâ€Earth Nanoparticles with Enhanced Upconversion Emission and Suppressed Rareâ€Earthâ€Ion Leakage. Chemistry - A European Journal, 2012, 18, 5558-5564.	1.7	195
101	Triple-functional core–shell structured upconversion luminescent nanoparticles covalently grafted with photosensitizer for luminescent, magnetic resonance imaging and photodynamic therapy in vitro. Nanoscale, 2012, 4, 4611.	2.8	209
102	Photoswitchable Upconversion Luminescence of Rareâ€Earth Nanophosphors with Covalently Grafted Spiropyran. Chemistry - an Asian Journal, 2012, 7, 2225-2229.	1.7	23
103	Ytterbium stabilized ordered mesoporous titania for near-infrared photocatalysis. Chemical Communications, 2011, 47, 8109.	2.2	81
104	Role of Surface Ligands in the Nanoparticle Assemblies: A Case Study of Regularly Shaped Colloidal Crystals Composed of Sodium Rare Earth Fluoride. Langmuir, 2011, 27, 3343-3347.	1.6	23
105	Fabrication and Characterization of Rare-Earth-Doped Nanostructures on Surfaces. ACS Nano, 2011, 5, 6539-6545.	7.3	44
106	Heteroepitaxial Growth of High-Index-Faceted Palladium Nanoshells and Their Catalytic Performance. Journal of the American Chemical Society, 2011, 133, 1106-1111.	6.6	287
107	Bioimaging and toxicity assessments of near-infrared upconversion luminescent NaYF4:Yb,Tm nanocrystals. Biomaterials, 2011, 32, 9059-9067.	5.7	239
108	Fluorescent-magnetic nanocrystals: synthesis and property of YPxV1â^'xO4:Eu@GdPO4 core/shell structure. Nanoscale, 2011, 3, 1977.	2.8	30

#	Article	IF	CITATIONS
109	Thermally Stable Pt/CeO ₂ Hetero-Nanocomposites with High Catalytic Activity. Journal of the American Chemical Society, 2010, 132, 4998-4999.	6.6	187
110	Synthesis and assembly of rare earth nanostructures directed by the principle of coordination chemistry in solution-based process. Coordination Chemistry Reviews, 2010, 254, 1038-1053.	9.5	150
111	Monazite and Zircon Type LaVO ₄ :Eu Nanocrystals – Synthesis, Luminescent Properties, and Spectroscopic Identification of the Eu ³⁺ Sites. European Journal of Inorganic Chemistry, 2010, 2010, 2626-2635.	1.0	63
112	Biocompatible Bright YVO ₄ :Eu Nanoparticles as Versatile Optical Bioprobes. Advanced Functional Materials, 2010, 20, 3708-3714.	7.8	151
113	Biocompatible Bright YVO4:Eu Nanoparticles as Versatile Optical Bioprobes. Advanced Functional Materials, 2010, 20, 3707-3707.	7.8	4
114	Luminescence Modulation of Ordered Upconversion Nanopatterns by a Photochromic Diarylethene: Rewritable Optical Storage with Nondestructive Readout. Advanced Materials, 2010, 22, 633-637.	11.1	192
115	Plasmon–molecule interactions. Nano Today, 2010, 5, 494-505.	6.2	193
116	Rare earth upconversion nanophosphors: synthesis, functionalization and application as biolabels and energy transfer donors. Journal of Rare Earths, 2010, 28, 807-819.	2.5	105
117	Heteroepitaxial Growth of Core–Shell and Core–Multishell Nanocrystals Composed of Palladium and Gold. Small, 2010, 6, 2566-2575.	5.2	94
118	Assembly of upconversion NaREF <inf>4</inf> nanocrystals. , 2010, , .		0
119	Colloidal synthesis and blue based multicolor upconversion emissions of size and composition controlled monodisperse hexagonal NaYF4 : Yb,Tm nanocrystals. Nanoscale, 2010, 2, 953.	2.8	221
120	Ionic Liquid-Based Route to Spherical NaYF4 Nanoclusters with the Assistance of Microwave Radiation and Their Multicolor Upconversion Luminescence. Langmuir, 2010, 26, 8797-8803.	1.6	91
121	Superparamagnetic and upconversion emitting Fe3O4/NaYF4 : Yb,Er hetero-nanoparticles via a crosslinker anchoring strategy. Chemical Communications, 2010, 46, 5731.	2.2	101
122	Luminescence resonance energy transfer based on β-NaYF4:Yb,Er nanoparticles and TRITC dye. Science in China Series B: Chemistry, 2009, 52, 1590-1595.	0.8	15
123	Functional-template directed self-assembly (FTDSA) of mesostructured organic-inorganic hybrid materials. Science in China Series B: Chemistry, 2009, 52, 1759-1768.	0.8	1
124	Plasmon Coupling in Clusters Composed of Twoâ€Đimensionally Ordered Gold Nanocubes. Small, 2009, 5, 2111-2119.	5.2	119
125	Solidâ€ŧoâ€Hollow Singleâ€Particle Manipulation of a Selfâ€Assembled Luminescent NaYF ₄ :Yb,Er Nanocrystal Monolayer by Electronâ€Beam Lithography. Small, 2009, 5, 2057-2060.	5.2	59
126	Controlled synthesis and assembly of ceria-based nanomaterials. Journal of Colloid and Interface Science, 2009, 335, 151-167.	5.0	229

#	Article	IF	CITATIONS
127	Growth of Tetrahexahedral Gold Nanocrystals with High-Index Facets. Journal of the American Chemical Society, 2009, 131, 16350-16351.	6.6	357
128	Atomically Efficient Synthesis of Self-assembled Monodisperse and Ultrathin Lanthanide Oxychloride Nanoplates. Journal of the American Chemical Society, 2009, 131, 3162-3163.	6.6	86
129	Highly Luminescent Self-Organized Sub-2-nm EuOF Nanowires. Journal of the American Chemical Society, 2009, 131, 16364-16365.	6.6	119
130	Self-Assembled Ferromagnetic Monodisperse Manganese Oxide Nanoplates Synthesized by a Modified Nonhydrolytic Approach. Journal of Physical Chemistry C, 2009, 113, 6521-6528.	1.5	15
131	Mesostructured Hybrids Containing Potential Donors and Acceptors with Molecular-Scale and Meso-Scale Segregation and Ordering: Toward the Development of Smart Materials through Hierarchical Self-Assembly. Chemistry of Materials, 2009, 21, 4589-4597.	3.2	18
132	Luminescent Properties in Relation to Controllable Phase and Morphology of LuBO3:Eu3+ Nano/Microcrystals Synthesized by Hydrothermal Approach. Chemistry of Materials, 2009, 21, 468-475.	3.2	80
133	Optically active uniform potassium and lithium rare earth fluoride nanocrystals derived from metal trifluroacetate precursors. Dalton Transactions, 2009, , 8574.	1.6	113
134	Ag nanowires enhanced upconversion emission of NaYF4:Yb,Er nanocrystals via a direct assembly method. Chemical Communications, 2009, , 4393.	2.2	199
135	Uniform Alkaline Earth Fluoride Nanocrystals with Diverse Shapes Grown from Thermolysis of Metal Trifluoroacetates in Hot Surfactant Solutions. Crystal Growth and Design, 2009, 9, 2013-2019.	1.4	83
136	Near-Infrared to Visible Upconversion in Er ³⁺ and Yb ³⁺ Codoped Lu ₂ O ₃ Nanocrystals: Enhanced Red Color Upconversion and Three-Photon Process in Green Color Upconversion. Journal of Physical Chemistry C, 2009, 113, 4413-4418.	1.5	119
137	Reversible luminescence switching of NaYF4:Yb,Er nanoparticles with controlled assembly of gold nanoparticles. Chemical Communications, 2009, , 2547.	2.2	63
138	Colour modification action of an upconversion photonic crystal. Chemical Communications, 2009, , 6616.	2.2	62
139	Strong Polarization Dependence of Plasmon-Enhanced Fluorescence on Single Gold Nanorods. Nano Letters, 2009, 9, 3896-3903.	4.5	388
140	Sol–gel synthesis of nanosized Y3Sc2.5Ga2.5O12 garnet. Mendeleev Communications, 2008, 18, 251-252.	0.6	4
141	Microscopic studies of a SnO2∫î±-Fe2O3 architectural nanocomposite using Mössbauer spectroscopic and magnetic measurements. Journal of Solid State Chemistry, 2008, 181, 3283-3286.	1.4	4
142	Size-dependent microstructure and europium site preference influence fluorescent properties of Eu3+-doped Ca10(PO4)6(OH)2 nanocrystal. Journal of Luminescence, 2008, 128, 428-436.	1.5	65
143	Luminescent rare earth nanomaterials for bioprobe applications. Dalton Transactions, 2008, , 5687.	1.6	367
144	Luminescence Resonance Energy Transfer Sensors Based on the Assemblies of Oppositely Charged Lanthanide/Gold Nanoparticles in Aqueous Solution. Chemistry - an Asian Journal, 2008, 3, 1857-1864.	1.7	26

#	Article	IF	CITATIONS
145	Resonance Energy Transfer in Steady-State and Time-Decay Fluoro-Immunoassays for Lanthanide Nanoparticles Based on Biotin and Avidin Affinity. Journal of Physical Chemistry C, 2008, 112, 6589-6593.	1.5	66
146	Facile Synthesis for Ordered Mesoporous Î ³ -Aluminas with High Thermal Stability. Journal of the American Chemical Society, 2008, 130, 3465-3472.	6.6	616
147	Room Temperature Ionic Liquids Assisted Green Synthesis of Nanocrystalline Porous SnO ₂ and Their Gas Sensor Behaviors. Crystal Growth and Design, 2008, 8, 4165-4172.	1.4	114
148	Sustainable and Facile Route to Nearly Monodisperse Spherical Aggregates of CeO ₂ Nanocrystals with Ionic Liquids and Their Catalytic Activities for CO Oxidation. Journal of Physical Chemistry C, 2008, 112, 18405-18411.	1.5	101
149	Incorporation of Gold Nanorods and Their Enhancement of Fluorescence in Mesostructured Silica Thin Films. Journal of Physical Chemistry C, 2008, 112, 18895-18903.	1.5	52
150	Efficient Energy Transfer in Monodisperse Eu-Doped ZnO Nanocrystals Synthesized from Metal Acetylacetonates in High-Boiling Solvents. Journal of Physical Chemistry C, 2008, 112, 12234-12241.	1.5	212
151	Large-Scale Synthesis of Single-Crystalline Iron Oxide Magnetic Nanorings. Journal of the American Chemical Society, 2008, 130, 16968-16977.	6.6	438
152	Luminescent Monodisperse Nanocrystals of Lanthanide Oxyfluorides Synthesized from Trifluoroacetate Precursors in High-Boiling Solvents. Journal of Physical Chemistry C, 2008, 112, 405-415.	1.5	130
153	Branched Gold Nanochains Facilitated by Polyvinylpyrrolidone and their SERS Effects on <i>p</i> -Aminothiophenol. Journal of Physical Chemistry C, 2008, 112, 16011-16016.	1.5	51
154	Hierarchical Construction of ZnO Architectures Promoted by Heterogeneous Nucleation. Crystal Growth and Design, 2008, 8, 3609-3615.	1.4	81
155	Orderly Aligned and Highly Luminescent Monodisperse Rare-Earth Orthophosphate Nanocrystals Synthesized by a Limited Anion-Exchange Reaction. Chemistry of Materials, 2007, 19, 4514-4522.	3.2	109
156	Size- and Phase-Controlled Synthesis of Monodisperse NaYF ₄ :Yb,Er Nanocrystals from a Unique Delayed Nucleation Pathway Monitored with Upconversion Spectroscopy. Journal of Physical Chemistry C, 2007, 111, 13730-13739.	1.5	256
157	Highly Efficient Multicolor Up-Conversion Emissions and Their Mechanisms of Monodisperse NaYF ₄ :Yb,Er Core and Core/Shell-Structured Nanocrystals. Journal of Physical Chemistry C, 2007, 111, 13721-13729.	1.5	580
158	Controlled-Synthesis, Self-Assembly Behavior, and Surface-Dependent Optical Properties of High-Quality Rare-Earth Oxide Nanocrystals. Chemistry of Materials, 2007, 19, 18-27.	3.2	171
159	Ordered Mesoporous Ce1-xZrxO2Solid Solutions with Crystalline Walls. Journal of the American Chemical Society, 2007, 129, 6698-6699.	6.6	171
160	Glutathione- and Cysteine-Induced Transverse Overgrowth on Gold Nanorods. Journal of the American Chemical Society, 2007, 129, 6402-6404.	6.6	178
161	Nanonecklaces assembled from gold rods, spheres, and bipyramids. Chemical Communications, 2007, , 1816.	2.2	146
162	Iron Oxide Tube-in-Tube Nanostructures. Journal of Physical Chemistry C, 2007, 111, 13022-13027.	1.5	98

#	Article	IF	CITATIONS
163	One-Step Synthesis of Large-Aspect-Ratio Single-Crystalline Gold Nanorods by Using CTPAB and CTBAB Surfactants. Chemistry - A European Journal, 2007, 13, 2929-2936.	1.7	94
164	Site selective excitation in La2O3:Eu3+ nanoparticles. Journal of Luminescence, 2007, 122-123, 844-846.	1.5	26
165	Surface state analysis of YVO4:Eu3+ nanocrystals by electrostatic point charge model. Journal of Luminescence, 2007, 122-123, 847-850.	1.5	4
166	Single-Crystalline and Near-Monodispersed NaMF3 (M=Mn, Co, Ni, Mg) and LiMAlF6 (M=Ca, Sr) Nanocrystals from Cothermolysis of Multiple Trifluoroacetates in Solution. Chemistry - an Asian Journal, 2007, 2, 965-974.	1.7	57
167	Size-controllable one-dimensinal SnO2 nanocrystals: synthesis, growth mechanism, and gas sensing property. Physical Chemistry Chemical Physics, 2006, 8, 4874.	1.3	85
168	High-Quality Sodium Rare-Earth Fluoride Nanocrystals:  Controlled Synthesis and Optical Properties. Journal of the American Chemical Society, 2006, 128, 6426-6436.	6.6	1,374
169	Growth of Gold Nanorods and Bipyramids Using CTEAB Surfactant. Journal of Physical Chemistry B, 2006, 110, 16377-16383.	1.2	127
170	Optical properties of ZnO nanoplatelets and rectangular cross-sectioned nanowires. Chemical Physics Letters, 2006, 422, 46-50.	1.2	22
171	Single-Crystalline Iron Oxide Nanotubes. Angewandte Chemie - International Edition, 2005, 44, 4328-4333.	7.2	494
172	Selective Synthesis of Monazite- and Zircon-Type LaVO4 Nanocrystals ChemInform, 2005, 36, no.	0.1	0
173	Single-Crystalline Iron Oxide Nanotubes ChemInform, 2005, 36, no.	0.1	1
174	Selective Synthesis of Monazite- and Zircon-type LaVO4Nanocrystals. Journal of Physical Chemistry B, 2005, 109, 3284-3290.	1.2	139
175	Hierarchical Assembly of SnO2Nanorod Arrays on α-Fe2O3Nanotubes: A Case of Interfacial Lattice Compatibility. Journal of the American Chemical Society, 2005, 127, 13492-13493.	6.6	212
176	Shape-Selective Synthesis and Oxygen Storage Behavior of Ceria Nanopolyhedra, Nanorods, and Nanocubes. Journal of Physical Chemistry B, 2005, 109, 24380-24385.	1.2	1,326
177	Attachment-Driven Morphology Evolvement of Rectangular ZnO Nanowires. Journal of Physical Chemistry B, 2005, 109, 8786-8790.	1.2	85
178	Structural transformation induced improved luminescent properties for LaVO4:Eu nanocrystals. Applied Physics Letters, 2004, 84, 5305-5307.	1.5	142
179	Ordered Nanosheet-Based YBO3:Eu3+ Assemblies: Synthesis and Tunable Luminescent Properties ChemInform, 2004, 35, no.	0.1	0
180	Ordered Nanosheet-Based YBO3:Eu3+Assemblies:Â Synthesis and Tunable Luminescent Properties. Journal of Physical Chemistry B, 2004, 108, 3387-3390.	1.2	115

#	Article	IF	CITATIONS
181	Acetate-Mediated Growth of Drumlike YBO3:Eu3+Crystals. Crystal Growth and Design, 2004, 4, 517-520.	1.4	73
182	Shape Evolution of One-Dimensional Single-Crystalline ZnO Nanostructures in a Microemulsion System. Crystal Growth and Design, 2004, 4, 309-313.	1.4	67
183	Structure transition and enhanced photoluminescence of Gd 2â^'x Y x O 3 :Eu nanocrystals. Journal of Solid State Chemistry, 2003, 171, 304-307.	1.4	42
184	Hydrothermal homogeneous urea precipitation of hexagonal YBO3:Eu3+ nanocrystals with improved luminescent properties. Journal of Solid State Chemistry, 2003, 175, 245-251.	1.4	118
185	Correlation between Size-Dependent Luminescent Properties and Local Structure around Eu3+ Ions in YBO3:Eu Nanocrystals:  An XAFS Study. Chemistry of Materials, 2003, 15, 3011-3017.	3.2	64
186	Size dependence of luminescent properties for hexagonal YBO3:Eu nanocrystals in the vacuum ultraviolet region. Journal of Applied Physics, 2003, 93, 9783-9788.	1.1	66
187	Eu3+ ion as fluorescent probe for detecting the surface effect in nanocrystals. Applied Physics Letters, 2003, 82, 3511-3513.	1.5	119
188	Fluorescence intensity and color purity improvement in nanosized YBO3:Eu. Applied Physics Letters, 2002, 80, 1447-1449.	1.5	177
189	Size-Dependent Chromaticity in YBO3:Eu Nanocrystals:  Correlation with Microstructure and Site Symmetry. Journal of Physical Chemistry B, 2002, 106, 10610-10617.	1.2	244
190	ZnO nanowires fabricated by a convenient route. New Journal of Chemistry, 2002, 26, 33-34.	1.4	153
191	A simple route towards tubular ZnO. Chemical Communications, 2002, , 262-263.	2.2	254
192	Synthesis and size dependent luminescent properties of hexagonal (Y,Gd)BO3â^¶Eu nanocrystals. Journal of Materials Chemistry, 2002, 12, 3665-3670.	6.7	45
193	Size control and photoluminescence enhancement of CdS nanoparticles prepared via reverse micelle method. Solid State Communications, 2002, 124, 45-48.	0.9	95
194	Fabrication of size controllable YVO4 nanoparticles via microemulsion-mediated synthetic process. Solid State Communications, 2002, 124, 35-38.	0.9	108
195	Control of ZnO Morhpology by Solution Route. Materials Research Society Symposia Proceedings, 2001, 692, 1.	0.1	0
196	Preparation of CdS/ZnO Core/shell Structured Nanoparticles by Hydrothermal Method. Materials Research Society Symposia Proceedings, 2001, 692, 1.	0.1	1
197	Carboxylic-containing copolymer as template to prepare CdS, ZnS and doped nanoparticles. Science in China Series B: Chemistry, 2001, 44, 23-30.	0.8	6
198	Synthesis and optical properties of nanosized CdS prepared in a quaternary CTAB/ nhexanol/n-heptane/water reverse micelle. Science Bulletin, 2001, 46, 1873-1877.	1.7	17

#	Article	IF	CITATIONS
199	Luminescent properties of Li+ doped nanosized Y2O3:Eu. Solid State Communications, 2001, 119, 393-396.	0.9	139
200	Rare earth activated nanosized oxide phosphors: synthesis and optical properties. Journal of Luminescence, 2000, 87-89, 447-450.	1.5	92